

Analog Superconducting Quantum Simulator for Holstein Polarons

Feng Mei¹, Vladimir M. Stojanović^{2,3}, Irfan Siddiqi⁴, and Lin Tian¹

¹*School of Natural Sciences, University of California, Merced, CA 95343, USA*

²*Department of Physics, University of Basel, Klingelbergstrasse 82, CH-4056 Basel, Switzerland*

³*Department of Physics, Harvard University, Cambridge, MA 02138, USA*

⁴*Quantum Nanoelectronics Laboratory, Department of Physics, University of California, Berkeley, CA 94720, USA*

We propose an analog quantum simulator for the Holstein molecular-crystal model based on a superconducting circuit QED system in the dispersive regime. By varying the driving field on the superconducting resonators, one can readily access both the adiabatic and anti-adiabatic regimes of this model. Strong e-ph coupling required for small-polaron formation can also be reached. We show that small-polaron state of arbitrary quasimomentum can be generated by applying a microwave pulse to the resonators. We also show that significant squeezing in the resonator modes can be achieved in the polaron-crossover regime through a measurement-based scheme.

PACS numbers: 85.25.Cp, 03.67.Ac, 71.38.Ht

I. INTRODUCTION

Quantum simulation of many-body systems opens up an exciting perspective for studying condensed matter and high energy effects that cannot be studied by traditional theoretical or experimental techniques.^{1,2} Owing to recent progress in quantum devices, the realization of quantum simulators for a broad spectrum of problems, such as quantum magnetism and quantum Hall effects, has been intensively studied.³ At the same time, the questions of how to exploit the unique features of each specific physical system to probe and manipulate the many-body state and the dynamics of the simulator remain to be answered.

The Holstein molecular-crystal model is commonly used to study the short-range coupling between fermionic excitation (electron, hole) and optical phonons (e-ph coupling).⁴ The coupling in this model has the form of a local interaction between the fermion density and the lattice displacement, and has important consequences on the optical and transport properties of the solids.⁵ One of the most fundamental many-body effects due to this coupling is the formation of a small polaron where an extra charge carrier becomes heavily dressed in a cloud of virtual phonons of the host crystal.⁶ The Holstein model does not admit analytical solution and can only be solved approximately by numerical methods. A quantum simulator for this model can advance our understanding of the behavior of polaronic systems. This simple many-body system can also give us hands-on experience in effectively manipulating quantum simulators built from a specific architecture. In previous works, simulators for the Holstein- and related models were proposed with cold polar molecules⁷ and trapped ions.^{8,9} However, the accessible parameter regimes and the effectiveness of these simulators are limited by intrinsic physical and technical constraints in these systems.

The flexibility and control of superconducting (SC) quantum circuits provide us with an excellent platform for quantum simulation.^{10,11} It was shown that quantum

spin systems can be simulated with SC qubits that have demonstrated ever increasing coherence times.¹² SC resonators are ideal for simulating bosonic degrees of freedoms such as phonons. The strong qubit-resonator coupling demonstrated in circuit quantum electrodynamics (circuit QED) experiments^{13,14} adds a Hubbard-like interaction for the microwave photons in the resonators and can be used to study quantum phase transitions in such systems.^{15,16} The diversity of the SC devices also enables the simulation of complex quantum processes such as universal quantum computation and exciton transport.¹⁷ Here, we propose an analog SC quantum simulator for the one-dimensional Holstein model. The central building block of our simulator is a circuit QED system composed of a transmon qubit and a SC resonator and operated in the dispersive regime.¹⁸ The role of the qubits is to simulate fermionic excitations and the resonator modes almost perfectly mimic Einstein phonons. The only tunable parameters required for accessing both the adiabatic and anti-adiabatic regimes and for preparing a small-polaron state of arbitrary quasimomentum are the amplitude and frequency of the microwave drive on the resonators. The coupling strength required for small-polaron formation can be readily reached. A striking feature of this simulator is that measurement-based squeezing up to 1.25 dB in the resonator modes can be achieved in the polaron state in the crossover regime. Meanwhile, detection of the polaron states can be achieved through an ancilla qubit (probe qubit) that couples with one of the resonator modes. Compared with previous proposals for the Holstein model,⁷⁻⁹ our proposal effectively simulates this model with essentially dispersionless phonons and hopping processes via Josephson couplings which naturally have nearest-neighbor character.

This paper is organized as the following. In Sec. II, we present a circuit-QED-based superconducting quantum simulator for the Holstein model and derive the many-body Hamiltonian for this system. By applying the Jordan-Wigner transformation, this Hamiltonian can be exactly mapped to the Holstein model. The accessi-

ble parameter regimes of this simulator are studied in Sec. III. Using a variational method, we show that small-polaron formation under strong e-ph coupling can be achieved with practical circuit parameters. In Sec. IV, we present a scheme that can prepare the simulator state into a polaron state with arbitrary quasimomentum. The anomalous amplitude fluctuation and momentum squeezing in the polaron ground state are studied in Sec. V. In Sec. VI, we discuss the detection of the polaron state. We also study the effects of decoherence and quantum leakage on the quantum simulator. Conclusions are given in Sec. VII.

II. THE SIMULATOR

The repeating unit of this simulator is made of a transmon qubit denoted by Q_n capacitively coupled with a SC resonator denoted by R_n , as is shown in Fig. 1. The resonators can be in various forms such as coplanar waveguide or lumped element resonators. The Hamiltonian of the repeating unit is described by the Jaynes-Cummings model

$$H_0^n = \hbar\omega_c a_n^\dagger a_n + \frac{\hbar\omega_z}{2} \sigma_n^z + \hbar g (a_n^\dagger \sigma_n^- + \sigma_n^+ a_n), \quad (1)$$

where ω_c and ω_z are the frequencies of the resonator and qubit respectively, g is the magnitude of the qubit-resonator coupling, a_n is the annihilation operator of the resonator mode, and $\sigma_n^{z,\pm}$ are the Pauli operators of the qubit. Adjacent qubits couple via a SQUID loop denoted by J_n with effective Josephson energy E_J . The coupling Hamiltonian is $H_J^n = -E_J \cos(\varphi_n - \varphi_{n+1})$ in terms of the gauge-invariant phases.¹⁹ For transmon qubits, we can write

$$H_J^n \approx -t_0 (\sigma_n^+ \sigma_{n+1}^- + \sigma_{n+1}^+ \sigma_n^-) \quad (2)$$

with hopping matrix element $t_0 = E_J \delta\phi_0^2$ and quantum displacement $\delta\phi_0$ of the phase variables (see Appendix A for details). In addition, the resonators are driven by a microwave source which is described by the Hamiltonian

$$H_d^n = 2\varepsilon_0 \cos(\omega_d t) (a_n + a_n^\dagger) \quad (3)$$

with driving amplitude ε_0 and driving frequency ω_d . The total Hamiltonian of this simulator is hence $H_t = \sum_n (H_0^n + H_J^n + H_d^n)$.

In the dispersive regime of $|\Delta| \gg g$ with $\Delta \equiv \omega_c - \omega_z$ being the qubit-resonator detuning, we apply the unitary transformation

$$U = \prod_n e^{-\frac{g}{\Delta} (\sigma_n^+ a_n - a_n^\dagger \sigma_n^-)} \quad (4)$$

to the simulator Hamiltonian.¹³ The term H_0^n is transformed into

$$\bar{H}_0^n = \hbar\omega_c a_n^\dagger a_n + \frac{\hbar}{2} (\omega_z - \chi) \sigma_n^z - \hbar\chi \sigma_n^z a_n^\dagger a_n, \quad (5)$$

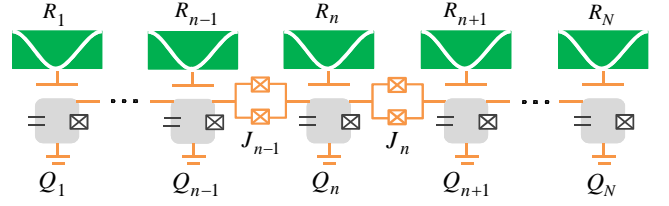


Figure 1: (Color online) Schematic setup of the SC simulator for the Holstein model with the transmon qubits denoted by Q_n , SC resonators denoted by R_n , and SQUID loops denoted by J_n .

with the Stark shift $\chi \equiv g^2/\Delta$. The terms H_J^n and H_d^n are also transformed accordingly. In the interaction picture and after a displacement of the resonator modes ($a_n \rightarrow a_n - \varepsilon_0/\hbar\delta\omega$), the total Hamiltonian becomes

$$\bar{H}_r = \sum_n \hbar\delta\omega \left[a_n^\dagger a_n + g_H \frac{\sigma_n^z + 1}{2} (a_n + a_n^\dagger) \right] + H_J^n \quad (6)$$

with $\delta\omega \equiv \omega_c + \chi - \omega_d$ and $g_H \delta\omega = 2\varepsilon_0 \chi/\hbar\delta\omega$. Note that we assume $\varepsilon_0 \gg \hbar\delta\omega$ in deriving this Hamiltonian. Details of the derivation of the above Hamiltonian can be found in Appendix A.

By applying the Jordan-Wigner transformation ($\sigma_n^+ \rightarrow c_n^\dagger \prod_{m=1}^{n-1} e^{i\pi c_m^\dagger c_m}$ and $\sigma_n^z = 2c_n^\dagger c_n - 1$), we derive

$$\bar{H}_r = \sum_n \hbar\delta\omega [a_n^\dagger a_n + g_H c_n^\dagger c_n (a_n + a_n^\dagger)] + \bar{H}_J^n \quad (7)$$

with $\bar{H}_J^n = -t_0 (c_n^\dagger c_{n+1} + c_{n+1}^\dagger c_n)$ and c_n being the annihilation operator of the fermionic excitations at site n . This Hamiltonian has the standard form of the Holstein model with $\delta\omega$, t_0 and g_H playing the roles of phonon frequency, nearest-neighbor hopping matrix element, and dimensionless e-ph coupling, respectively. Note that given the diversity of SC circuits, other types of SC qubits such as the flux qubit can also be used to construct a quantum simulator for the Holstein model. In Appendix B, we present a flux-qubit-based quantum simulator for this model.

III. POLARON CROSSOVER

By varying the driving parameters (ε_0 , ω_d), all interesting regimes of the Holstein model can be accessed where a fermionic excitation displays qualitatively different behavior. The adiabatic (anti-adiabatic) regime can be accessed by choosing $\hbar\delta\omega/t_0$ to be smaller (larger) than one. With $\lambda = g_H^2 \hbar\delta\omega/t_0$, the conditions for small-polaron formation are g_H , $\lambda > 1$. In Fig.2 (a) and (b), we plot g_H and λ at selected $\delta\omega$ values for a practical set of parameters: $g/2\pi = 200$ MHz, $\Delta/2\pi = 4$ GHz, and $t_0/2\pi\hbar = 80$ MHz. It can be seen that the crossover from quasi-free excitation to strongly-dressed small-polaron state can be realized in both the adiabatic and anti-adiabatic regimes. For example, at $\varepsilon_0/2\pi\hbar = 400$ MHz

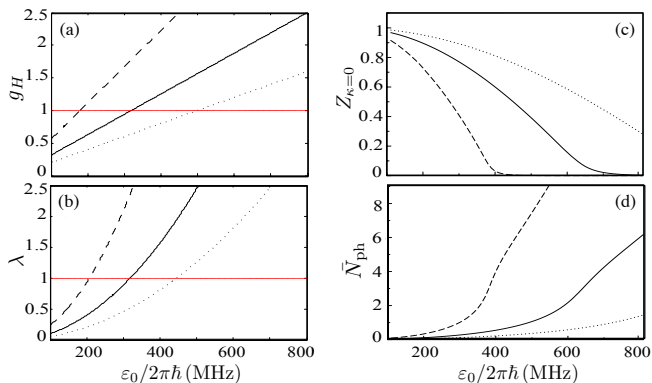


Figure 2: Dimensionless coupling constants (a) g_H and (b) λ , (c) Quasiparticle residue $Z_{\kappa=0}$, and (d) mean phonon number \bar{N}_{ph} versus driving amplitude ε_0 . The dashed, solid, and dotted curves are for $\hbar\delta\omega/t_0 = 0.75, 1, 1.25$, respectively.

and $\delta\omega/2\pi = 80$ MHz, we obtain $g_H = 1.25$ and $\lambda = 1.56$. Note that an optional control on the simulator is to tune the hopping matrix element t_0 by applying a global magnetic flux to the SQUID loops J_n , which can adjust the adiabaticity of the system.

To demonstrate the polaron crossover in the simulator, we apply a variational method to find the small-polaron ground state using the Toyozawa Ansatz which provides a rather accurate estimate of the ground-state energy of the Holstein model in all relevant physical regimes.²⁰ The ground state can be obtained by minimizing the energy expectation value with respect to the variational parameters in the Ansatz (see Appendix C for details). One important quantity for characterizing polaron excitation is the quasiparticle residue $Z_\kappa \equiv |\langle \Psi_{k=\kappa} | \tilde{\psi}_\kappa \rangle|^2$ which is defined as the overlap between the dressed polaron state $|\tilde{\psi}_\kappa\rangle$ at quasimomentum κ and the bare-excitation Bloch state $|\Psi_k\rangle \equiv c_k^\dagger |0\rangle$ at momentum $k = \kappa$ with $c_k = \sum_n c_n e^{ikn} / \sqrt{N}$. This quantity can characterize the crossover from the bare-excitation regime into the small-polaron regime. Another quantity characterizing the polaron crossover is the mean phonon number $\bar{N}_{ph} \equiv \langle \tilde{\psi}_{\kappa=0} | \sum_i a_i^\dagger a_i | \tilde{\psi}_{\kappa=0} \rangle$ in the polaron ground state. For the Toyozawa Ansatz, both Z_κ and \bar{N}_{ph} can be evaluated in terms of the optimal values of the variational parameters. In Fig.2 (c) and (d), these two quantities are shown using the parameter values given above for a system size of $N = 32$. The change of $Z_{\kappa=0}$ from unity to values very close to zero as ε_0 increases is a clear manifestation of the smooth crossover from a quasi-free excitation to a small polaron state. The same crossover is also illustrated by the mean phonon number which varies from nearly zero to $\bar{N}_{ph} \gtrsim 3$ as ε_0 increases. Note that we also calculate the above quantities for small systems of, e.g., $N = 4$ (which is easier to realize in experiments), and find nearly identical results due to the local nature of the lattice distortion in the small-polaron regime.

IV. POLARON-STATE PREPARATION

To study polaron crossover, extra fermionic excitation needs to be prepared in the simulator. Without this extra excitation, the many-body state can be written as $|G_0\rangle = |0\rangle_e \otimes |0\rangle_{ph}$ in the excitation-phonon basis. In the physical basis of the qubit-resonator system, this state has all the qubits in the spin down state and all the resonators in the vacuum state. In the SC circuit, this state can be prepared via thermalization in a low temperature environment. Here we show that given the initial state $|G_0\rangle$, a small-polaron state with arbitrary quasimomentum can be generated through a qubit-flip scheme.

Consider applying a pumping pulse on the resonators in the form of

$$H_p = \varepsilon_p(t) \sum (a_n^\dagger e^{-iqn} + a_n e^{iqn}) / \sqrt{N} \quad (8)$$

with time-dependent driving amplitude $\varepsilon_p(t)$ and wave vector q . After applying the transformation U given in Eq.(4) (with $U a_n U^\dagger \approx a_n - (g/\Delta)\sigma_n^-$),¹³ we obtain an effective pumping Hamiltonian on the qubits

$$\Omega(q, t) = \beta(t) \sum_n (\sigma_n^+ e^{-iqn} + \sigma_n^- e^{iqn}) / \sqrt{N}, \quad (9)$$

with $\beta(t) = -(g/\Delta)\varepsilon_p(t)$, which describes a spin-flip operation on the qubits with site-dependent factor e^{-iqn} . After the Jordan-Wigner transformation, we apply this operator to the state $|G_0\rangle$. With $c_n |G_0\rangle = 0$, we find that $\Omega(q, t)|G_0\rangle = \hbar\beta(t)c_q^\dagger|G_0\rangle$, generating a bare excitation of momentum q . Hence the transition matrix element can be written as $\langle \tilde{\psi}_\kappa | \Omega(q, t) | G_0 \rangle = \hbar\beta(t)\Omega_{q\kappa}$ with $\Omega_{q\kappa} = \langle \tilde{\psi}_\kappa | c_q^\dagger | G_0 \rangle$. Using the lattice translational symmetry of the system, we derive that

$$|\Omega_{q\kappa}| = \sqrt{Z_\kappa} \delta_{q,\kappa}, \quad (10)$$

yielding nonzero matrix element only for $q = \kappa$.

Let $\hbar\omega_p$ be equal to the energy difference between the state $|G_0\rangle$ and the polaron state $|\psi_\kappa\rangle$. By choosing $q = \kappa$ and $\beta(t) = 2\beta_p \cos(\omega_p t)$, and under the rotating wave approximation, the pumping in Eq.(9) generates a Rabi oscillation between the initial state $|G_0\rangle$ and the target state $|\tilde{\psi}_\kappa\rangle$. This oscillation is governed by the effective Hamiltonian

$$\bar{H}_p = \beta_p \left(\Omega_{\kappa\kappa} |\tilde{\psi}_\kappa\rangle \langle G_0| + \Omega_{\kappa\kappa}^* |G_0\rangle \langle \tilde{\psi}_\kappa| \right) \quad (11)$$

with a Rabi frequency $\beta_p |\Omega_{\kappa\kappa}|$. Starting from the state $|G_0\rangle$, the system evolves to the target state $|\tilde{\psi}_\kappa\rangle$ in a duration $\tau = \pi\hbar / (2\beta_p \sqrt{Z_\kappa})$. For the polaron state $|\tilde{\psi}_{\kappa=0}\rangle$, $Z_{\kappa=0}$ decreases with the increase of ε_0 as is shown in Fig.2 (c) and it takes a longer time to generate a strongly-dressed polaron state. For $\beta_p/2\pi\hbar = 20$ MHz and $Z_\kappa = 0.7$, the state preparation time is $\tau = 18$ ns. This corresponds to a practical value of $\varepsilon_p/2\pi\hbar = 400$ MHz with the parameters given previously.

In this process, the condition $q = \kappa$ ensures momentum conservation and the choice of the pumping frequency ensures energy conservation. This scheme can be generalized and applied to quantum simulators for other many-body systems to generate elementary excitations by exploiting the symmetry in these systems.

V. ANOMALOUS FLUCTUATION AND SQUEEZING

In the Holstein model, the interplay between the strong e-ph coupling and the hopping of the fermionic excitation can induce anomalous fluctuation in the phonon modes. In our simulator, this fluctuation occurs when the driving amplitude ε_0 increases to reach the crossover regime. We denote the variance of an operator A by $S_A = \langle (A - \langle A \rangle)^2 \rangle$. This quantity characterizes the fluctuation of the operator around its average value. For the position quadrature $x_n \equiv (a_n + a_n^\dagger)/\sqrt{2}$ and the momentum quadrature $p_n \equiv -i(a_n - a_n^\dagger)/\sqrt{2}$ of mode a_n , their variances S_x and S_p are shown in Fig.3 (a) and (b). The variance S_x is always larger than the quantum limit of $1/2$ and increases monotonically as ε_0 increases, which clearly demonstrates the crossover to the small-polaron regime. The variance S_p varies in a very narrow region below $1/2$ with the product $S_x S_p > 1/4$, reflecting the non-Gaussian nature of the fluctuation in the small-polaron state. Due to the lattice translational symmetry, these variances do not depend on the site index n .

The above variances can be viewed as the averaged fluctuation of the resonator modes by tracing out the fermionic excitation. Below we study the variances of a single resonator mode when the fermionic excitation is pinned at this site. Consider the measurement-based position and momentum quadratures

$$x^{(m)} \equiv \sum c_n^\dagger c_n (a_n + a_n^\dagger)/\sqrt{2}; \quad (12)$$

$$p^{(m)} \equiv -i \sum c_n^\dagger c_n (a_n - a_n^\dagger)/\sqrt{2}. \quad (13)$$

The variances of these quadratures $S_x^{(m)}$ and $S_p^{(m)}$ describe the fluctuation of the resonator mode a_n when the excitation (qubit-flip) is detected at this site. In Fig.3 (c) and (d), it can be seen that $S_x^{(m)} > 1/2$ and $S_p^{(m)} < 1/2$, a property they share with S_x and S_p . However, as ε_0 increases, $S_x^{(m)}$ behaves very differently from S_x and shows an optimal value in the crossover regime. More interestingly, the momentum quadrature $S_p^{(m)}$ can reach a low value of 0.35, i.e., the post-selected momentum quadrature of a_n can be squeezed by up to 1.25 dB when the polaron is detected at this site. For a finite array of N sites, the probability of measuring the polaron excitation at a single site is $1/N$. Our numerical results show that this behavior can be observed in a small array of only, e.g., $N = 4$ sites, with a probability of $1/4$, which can be readily realized with current technology. Hence, accessing the crossover regime in the simulator is not only a

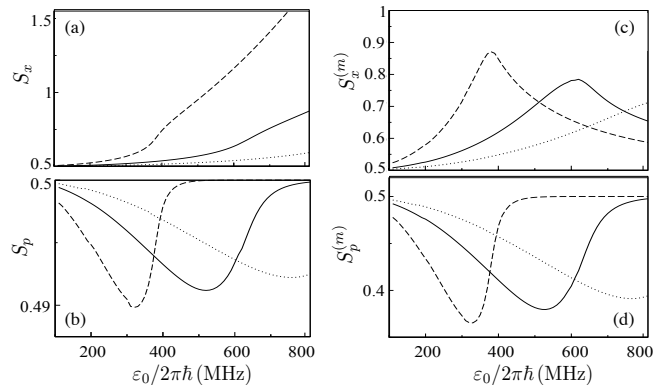


Figure 3: The variances of the resonator modes (a) S_x , (b) S_p , (c) $S_x^{(m)}$, and (d) $S_p^{(m)}$ versus ε_0 . The dashed, solid, and dotted curves are for $\hbar\delta\omega/t_0 = 0.75, 1, 1.25$ MHz, respectively.

crucial requirement to study the polaron formation, but also presents us with a novel approach to generate squeezing in the microwave photon modes of the resonators.²¹

VI. DETECTION AND DECOHERENCE

A crucial step in the quantum simulation of a many-body system is the detection of the many-body state. In a quantum simulator for the Holstein model, we can characterize the polaron crossover by measuring the mean phonon number \bar{N}_{ph} in the polaron ground state. Because of the lattice translational symmetry, this can be further simplified to the measurement of the mean phonon number of one of the resonators, e.g., a_1 . For this purpose, we add an ancilla qubit σ_d which couples to the resonator a_1 only during the measurement. The coupling is in the form of Eq.(1). When the qubit is far detuned from the resonator mode, the mean phonon number of a_1 can be obtained by measuring the Stark shift of the qubit. Note that in a different regime when the qubit is in resonance with the resonator mode, the mean phonon number can also be obtained by measuring the qubit. Besides the measurement of the ancilla qubit, in order to achieve the measurement-based squeezing in one of the resonator modes, measurement of the qubit at the same site is required.

The extra excitation in the simulator corresponds to a flipping of the qubit states and a displacement of the resonator modes which are subject to the decoherence of the qubits or the resonators. The coherence properties of SC qubits and resonators have improved significantly over the past few years. Decoherence time of transmon qubits coupling to on-chip resonators can now reach $10-40 \mu\text{s}$.²² For coplanar waveguide resonators, the damping time of the microwave photons can reach the same order of magnitude with a quality factor of $Q = 10^6$.²³ In our simulator, the effective phonon frequency, the e-ph coupling, and the hopping element are all of hundreds of mega-

hertz, far exceeding these decoherence rates. The duration of the state-preparation pulse is several orders of magnitude shorter than the decoherence times. In addition, thermal excitations can be neglected in the low temperature environment as the energy of the excitation is of a few gigahertz. The pump pulses may induce leakage (unwanted transitions) to higher energy levels in the transmon qubit.¹⁸ However, typical anharmonicity of a transmon qubit gives us an off resonance of around 500 MHz for the unwanted transitions. For a driving amplitude $\beta_p/2\pi = 25$ MHz, the probability of leakage is well below one percent, which is a tolerable error rate for the simulator.

VII. CONCLUSIONS

To conclude, we propose a circuit QED-based quantum simulator for the Holstein-polaron model. By varying the driving on the resonators, all relevant physical regimes of the Holstein model can be accessed, and in particular, we can reach the strong coupling regime for small-polaron formation. We also show that polaron state of arbitrary quasimomentum can be prepared by pumping the resonators. The polaron state in the crossover regime shows the striking feature of measurement-based squeezing in the resonator modes. Our work not only opens a promising route to study the electron-phonon physics with SC quantum simulators, but can also advance the control and detection methods for the many-body states in SC simulators by exploiting the unique controllability of such devices.

ACKNOWLEDGEMENTS

We thank Christoph Bruder for very helpful discussions. F. M. and L. T. were supported by NSF-DMR-0956064 and NSF-CCF-0916303. V. M. S. was supported by the SNSF and the NCCR QSIT. I. S. acknowledges partial support from the NSF Award 0939514. This research was supported in part by NSF PHY11-25915 through a KITP program.

APPENDIX A: DERIVATION OF THE EFFECTIVE HAMILTONIAN

The total Hamiltonian of the simulator is given by $H_t = \sum_n (H_0^n + H_J^n + H_d^n)$, where the terms H_0^n , H_J^n , and H_d^n are given in Eqs.(1-3). In the Josephson coupling $H_J^n = -E_J \cos(\varphi_n - \varphi_{n+1})$ between adjacent qubits, the effective Josephson energy of the SQUID loop can be written as $E_J = 2E_{J0} \cos(\pi\Phi_x/\Phi_0)$, where E_{J0} is the Josephson energy of the single junctions in the SQUID loop, Φ_x is the static magnetic flux in the loop, and Φ_0 is the flux quantum.¹⁹ By adjusting the magnetic flux in the SQUID loop, the effective Josephson energy can be

manipulated. For transmon qubits, H_J^n can be approximated as

$$H_J^n \approx E_J \delta\phi_0^2 \left[\frac{\sigma_n^z + \sigma_{n+1}^z}{2} - (\sigma_n^+ \sigma_{n+1}^- + \sigma_{n+1}^+ \sigma_n^-) \right], \quad (14)$$

where we have neglected the constant terms. Here, $\delta\phi_0$ is the quantum displacement of the phase variable φ_n with $\delta\phi_0^2 \sim \sqrt{2E_{C1}/E_{J1}}$ written in terms of the charging energy E_{C1} and the Josephson energy E_{J1} of the transmon qubit. With typical parameters, $\delta\phi_0^2 \sim 0.15$ ¹⁸. The first term in Eq.(14) can be absorbed into the qubit energy ω_z . Hence, the Josephson coupling can be simplified as $H_J^n = -t_0 (\sigma_n^+ \sigma_{n+1}^- + \sigma_{n+1}^+ \sigma_n^-)$ with hopping matrix element $t_0 = E_J \delta\phi_0^2$.

Our simulator is operated in the dispersive regime where the magnitude of the detuning far exceeds the magnitude of the qubit-resonator coupling, i.e., $|\Delta| \gg g$. Here the detuning is defined as $\Delta \equiv \omega_c - \omega_z$. We start by applying the unitary transformation U given in Eq.(4) to the total Hamiltonian H_t . The term H_0^n is transformed into $\bar{H}_0^n = UH_0^nU^\dagger$ given in Eq.(5) to the lowest order of the small ratio g/Δ with $\chi \equiv g^2/\Delta$ being the Stark shift. In a similar manner, we can derive the expressions for $UH_J^nU^\dagger$ and $UH_d^nU^\dagger$ and derive the transformed total Hamiltonian $\bar{H}_t = UH_tU^\dagger$.

For the transformed Hamiltonian, we consider the interaction picture defined by the non-interacting Hamiltonian

$$H_0 = \sum_n [\hbar\omega_d a_n^\dagger a_n + (\hbar\bar{\omega}_z/2)\sigma_n^z], \quad (15)$$

where $\bar{\omega}_z = \omega_z - \chi - 2\chi(\varepsilon_0/\hbar\delta\omega)^2$ is the modified qubit frequency and $\delta\omega = \omega_c + \chi - \omega_d$ is the modified resonator detuning. The modified qubit frequency $\bar{\omega}_z$ includes the Stark shift and another term that is used to balance the effect of the microwave driving. By applying the rotating wave approximation (RWA) and omitting the fast-rotating terms, the transformed Hamiltonian in the interaction picture can be written as

$$\bar{H}_{r1} = \sum_n [H_1^n + H_J^n + \varepsilon_0 (a_n + a_n^\dagger)]. \quad (16)$$

with the term

$$H_1^n = \hbar\delta\omega a_n^\dagger a_n + \hbar\chi \left(\frac{\varepsilon_0}{\hbar\delta\omega} \right)^2 \sigma_n^z - \hbar\chi (\sigma_n^z + 1) a_n^\dagger a_n. \quad (17)$$

Fast-rotating terms such as $a_n^\dagger \sigma_n^-$ generated by the transformation U have been omitted under the RWA. Next, we apply a displacement operator²⁴ to shift the resonator modes with $a_n \rightarrow a_n - \varepsilon_0/\hbar\delta\omega$. After this shift, the Hamiltonian \bar{H}_{r1} becomes \bar{H}_r in Eq.(6) with the coupling constant $g_H \delta\omega = 2\varepsilon_0\chi/\hbar\delta\omega$. With $\varepsilon_0 \gg \hbar\delta\omega$, the term $-\hbar\chi (\sigma_n^z + 1) a_n^\dagger a_n$ has been neglected from the above Hamiltonian. To convert the qubit modes to fermionic excitations, we apply the Jordan-Wigner transformation to the spin operators. The Hamiltonian \bar{H}_r then recovers the form in Eq.(7).

APPENDIX B: REALIZATION WITH FLUX QUBIT

Given the diversity of the SC circuits, quantum simulator for the Holstein-like model can also be realized with other SC qubits such as the flux qubit and the phase qubit. Here we present a realization of the Holstein model with the flux qubit.²⁵ We will show that a total Hamiltonian of the form $H_t = \sum_n (H_0^n + H_J^n + H_d^n)$ can be constructed with the flux qubit.

Consider a flux qubit biased at the degeneracy point (with a bias magnetic flux of $\Phi_{ex} = 0.5\Phi_0$). The qubit Hamiltonian can be written as $\hbar\omega_z\sigma_n^z/2$ in terms of the eigenstates, where $\hbar\omega_z$ is equal to the quantum tunneling between the two persistent-current states of the flux qubit and the eigenstates are 90 degrees rotated from the persistent-current states.²⁵ It was shown in recent experiments that the quantum tunneling can exceed a few gigahertz.²⁶ The microwave mode of the SC resonator couples to the flux qubit through its magnetic field which inductively couples to the current loop of the qubit and generates a coupling $g(a_n + a_n^\dagger)\sigma_n^x$. The magnitude of the coupling can be engineered in a very wide range and can readily reach sub-gigahertz.²⁷ The single-site Hamiltonian can hence be written as Eq.(1) under the RWA.

The neighboring qubits naturally couple via their mutual inductance. The coupling Hamiltonian can be written as $H_J^n = -t_0\sigma_n^x\sigma_{n+1}^x$, where $t_0 = MI_{cir}^2$ with M being the mutual inductance between the qubits and I_{cir} being the magnitude of the circulating current of the qubit states. Under the RWA, the coupling can be written as $H_J^n = -t_0(\sigma_n^+\sigma_{n+1}^- + \sigma_{n+1}^+\sigma_n^-)$ after neglecting the fast-rotating terms. One drawback of this coupling is its long-range nature, which induces coupling between qubits that are not immediately adjacent to each other. However, as the mutual inductance decreases as $1/r^3$ with r being an effective distance between two qubits, the coupling between non-neighboring qubits also decreases as $1/r^3$. An alternative coupling scheme is to design a tunable coupling between neighboring qubits, where the coupling can be controlled by external sources.

The resonators can be driven by a microwave source in

the form of H_d^n . Hence, combining all three terms: H_0^n , H_J^n , and H_d^n , we obtain a total Hamiltonian H_t with the flux qubit. Following the procedure presented in Appendix A, we can construct the Holstein model from this Hamiltonian. It can be shown that all relevant physical regimes can also be accessed in this realization.

APPENDIX C: TOYOZAWA ANSATZ

To determine the polaron ground state of our system, we make use of a variational method which yields results that agree well with quantum Monte Carlo and exact-diagonalization results. As the eigenstates of the Holstein Hamiltonian are good quasimomentum states, the variational states are Bloch-type states $|\psi_\kappa\rangle = N^{-1/2} \sum_n e^{-i\kappa n} |\psi_\kappa(n)\rangle$, where $|\psi_\kappa(n)\rangle$ denotes a Wannier-like function of the coupled e-ph system and κ is an eigenstate of the total quasimomentum operator $K = \sum_k k c_k^\dagger c_k + \sum_q q a_q^\dagger a_q$. Here we use the Toyozawa Ansatz state as our variational state.²⁰ This Ansatz state is given by

$$|\psi_\kappa(n)\rangle = \sum_{m=-N/2}^{N/2-1} \Phi_\kappa(m) e^{-i\kappa m} c_{n+m}^\dagger |0\rangle_e |\xi_\kappa(n)\rangle_{\text{ph}}, \quad (18)$$

where $|\xi_\kappa(n)\rangle_{\text{ph}} \equiv \prod_l \exp(v_l^\kappa a_{n+l}^\dagger - v_l^{\kappa*} a_{n+l}) |0\rangle_{\text{ph}}$ is a direct product of phonon coherent states at sites $n+l$ ($l = -N/2, \dots, N/2-1$) and the $2N$ variational parameters $\{\Phi_\kappa(m), v_l^\kappa\}$ are complex valued. Here c_n 's (a_m 's) are the real space operators of the fermionic excitations (phonons) at site n (m). This Ansatz provides a rather accurate estimate of the polaron ground-state energy of the Holstein model in all relevant physical regimes. The ground state can be obtained by minimizing the expectation value $\langle \psi_{\kappa=0} | H | \psi_{\kappa=0} \rangle / \langle \psi_{\kappa=0} | \psi_{\kappa=0} \rangle$ with respect to the variational parameters. We also introduce the normalized dressed excitation state at quasimomentum κ as $|\tilde{\psi}_\kappa\rangle = |\psi_\kappa\rangle / \sqrt{\langle \psi_\kappa | \psi_\kappa \rangle}$. In the main paper, we use the wave function $|\tilde{\psi}_\kappa\rangle$ in all our discussions.

¹ R. P. Feynman, Int. J. Theor. Phys. **21**, 467 (1982).

² S. Lloyd, Science **273**, 1073 (1996).

³ J. I. Cirac and P. Zoller, Nat. Phys. **8**, 264 (2012).

⁴ T. Holstein, Ann. Phys. (N.Y.) **8**, 343 (1959).

⁵ See, e.g., L. M. Woods and G. D. Mahan, Phys. Rev. B **61**, 10651 (2000); S. M. Badalyan and F. M. Peeters, *ibid.* **85**, 205453 (2012); K. Hannewald, V. M. Stojanović, and P. A. Bobbert, J. Phys.: Condens. Matter **16**, 2023 (2004); C.-H. Park, F. Giustino, M. L. Cohen, and S. G. Louie, Phys. Rev. Lett. **99**, 086804 (2007); N. Vukmirović, C. Bruder, and V. M. Stojanović, *ibid.* **109**, 126407 (2012); H. Ma, T. K. Lee, and Y. Chen, New J. Phys. **15**, 043045 (2013).

⁶ A. S. Alexandrov and J. T. Devreese, *Advances in Polaron*

Physics (Springer-Verlag, Berlin, 2010); J. Ranninger and U. Thibblin, Phys. Rev. B **45**, 7730 (1992); G. Wellein and H. Fehske, *ibid.* **56**, 4513 (1997); L.-C. Ku, S. A. Trugman, and J. Bonča, Phys. Rev. B **65**, 174306 (2002); V. M. Stojanović and M. Vanević, Phys. Rev. B **78**, 214301 (2008).

⁷ F. Herrera and R. V. Krems, Phys. Rev. A **84**, 051401(R) (2011); F. Herrera, K. W. Madison, R. V. Krems, and M. Berciu, Phys. Rev. Lett. **110**, 223002 (2013).

⁸ V. M. Stojanović, T. Shi, C. Bruder, and J. I. Cirac, Phys. Rev. Lett. **109**, 250501 (2012).

⁹ A. Mezzacapo, J. Casanova, L. Lamata, and E. Solano, Phys. Rev. Lett. **109**, 200501 (2012).

¹⁰ M. H. Devoret and R. J. Schoelkopf, Science **339**, 1169

- (2013); J. Q. You and F. Nori, *Nature (London)* **474**, 589 (2011); J. Clarke and F. K. Wilhelm, *Nature (London)* **453**, 1031 (2008); Y. Makhlin, G. Schön, and A. Shnirman, *Rev. Mod. Phys.* **73**, 357 (2001).
- ¹¹ See, e.g., M. D. Reed, L. DiCarlo, S. E. Nigg, L. Sun, L. Frunzio, S. M. Girvin, and R. J. Schoelkopf, *Nature (London)* **482**, 382 (2012); E. Lucero, R. Barends, Y. Chen, J. Kelly, M. Mariantoni, A. Megrant, P. O’Malley, D. Sank, A. Vainsencher, J. Wenner, T. White, Y. Yin, A. N. Cleland, and J. M. Martinis, *Nat. Phys.* **8**, 719 (2012); R. Vijay, C. Macklin, D. H. Slichter, S. J. Weber, K. W. Murch, R. Naik, A. N. Korotkov, and I. Siddiqi, *Nature (London)* **490**, 77 (2012); M. Mariantoni, H. Wang, T. Yamamoto, M. Neeley, R. C. Bialczak, Y. Chen, M. Lenander, E. Lucero, A. D. O’Connell, D. Sank, M. Weides, J. Wenner, Y. Yin, J. Zhao, A. N. Korotkov, A. N. Cleland, and J. M. Martinis, *Science* **334**, 61 (2011); A. Fedorov, L. Steffen, M. Baur, M. P. da Silva, and A. Wallraff, *Nature (London)* **481**, 170 (2011); F. Deppe, M. Mariantoni, E. P. Menzel, A. Marx, S. Saito, K. Kakuyanagi, H. Tanaka, T. Meno, K. Semba, H. Takayanagi, E. Solano, and R. Gross, *Nat. Phys.* **4**, 686 (2008).
- ¹² J. J. García-Ripoll, E. Solano, and M. A. Martin-Delgado, *Phys. Rev. B* **77**, 024522 (2008); L. Tian, *Phys. Rev. Lett.* **105**, 167001 (2010); S. Gammelmark and K. Mølmer, *New J. Phys.* **13**, 053035 (2011); *Phys. Rev. A* **85**, 042114 (2012); H. Ian, Y.-X. Liu, and F. Nori, *Phys. Rev. A* **85**, 053833 (2012); O. Viehmann, J. von Delft, and F. Marquardt, *Phys. Rev. Lett.* **110**, 030601 (2013).
- ¹³ A. Blais, R. S. Huang, A. Wallraff, S. M. Girvin, and R. J. Schoelkopf, *Phys. Rev. A* **69**, 062320 (2004); J. Q. You and F. Nori, *Phys. Rev. B* **68**, 064509 (2003); F. Marquardt and C. Bruder, *Phys. Rev. B* **63**, 054514 (2001).
- ¹⁴ A. Wallraff, D. I. Schuster, A. Blais, L. Frunzio, R.-S. Huang, J. Majer, S. Kumar, S. M. Girvin, and R. J. Schoelkopf, *Nature* **431**, 162 (2004).
- ¹⁵ M. J. Hartmann, F. G. S. L. Brandao, and M. B. Plenio, *Laser Photon. Rev.* **2**, 527 (2008); A. A. Houck, H. E. Türeci, and J. Koch, *Nature Phys.*, **8**, 292 (2012).
- ¹⁶ J. Koch and K. Le Hur, *Phys. Rev. A* **80**, 023811 (2009); D. I. Tsomokos, S. Ashhab, and F. Nori, *Phys. Rev. A* **82**, 052311 (2010); Y. Hu and L. Tian, *Phys. Rev. Lett.* **106**, 257002 (2011); A. L. C. Hayward, A. M. Martin, and A. D. Greentree, *Phys. Rev. Lett.* **108**, 223602 (2012); B. Peropadre, D. Zueco, F. Wulschner, F. Deppe, A. Marx, R. Gross, and J. J. García-Ripoll, *Phys. Rev. B* **87**, 134504 (2013); J. S. Pedernales, R. Di Candia, D. Ballester, and E. Solano, *New J. Phys.* **15**, 055008 (2013).
- ¹⁷ M. R. Geller, J. M. Martinis, A. T. Sornborger, P. C. Stancil, E. J. Pritchett, and A. Galiutdinov, arXiv:1210.5260; S. Mostame, P. Rebentrost, A. Eisfeld, A. J. Kerman, D. I. Tsomokos, and A. Aspuru-Guzik, *New J. Phys.* **14**, 105013 (2012); C.P. Meaney, T. Duty, R. H. McKenzie, and G. J. Milburn, *Phys. Rev. A* **81**, 043805 (2010); J. Larson, *Phys. Rev. A* **78**, 033833 (2008).
- ¹⁸ J. Koch, T. M. Yu, J. Gambetta, A. A. Houck, D. I. Schuster, J. Majer, A. Blais, M. H. Devoret, S. M. Girvin, and R. J. Schoelkopf, *Phys. Rev. A* **76**, 042319 (2007).
- ¹⁹ T.P. Orlando and K.A. Delin, *Foundations of Applied Superconductivity* (Addison Wesley, 1991).
- ²⁰ Y. Toyozawa, *Prog. Theor. Phys.* **26**, 29 (1961).
- ²¹ K. Moon and S.M. Girvin, *Phys. Rev. Lett.* **95**, 140504 (2005); M. Marthaler, G. Schön, and A. Shnirman, *Phys. Rev. Lett.* **101**, 147001 (2008).
- ²² H. Paik, D. I. Schuster, L. S. Bishop, G. Kirchmair, G. Catelani, A. P. Sears, B. R. Johnson, M. J. Reagor, L. Frunzio, L. I. Glazman, S. M. Girvin, M. H. Devoret, and R. J. Schoelkopf, *Phys. Rev. Lett.* **107**, 240501 (2011); C. Rigetti, J. M. Gambetta, S. Poletto, B. L. T. Plourde, J. M. Chow, A. D. Córcoles, J. A. Smolin, S. T. Merkel, J. R. Rozen, G. A. Keefe, M. B. Rothwell, M. B. Ketchen and M. Steffen, *Phys. Rev. B* **86**, 100506(R) (2012); R. Barends, J. Kelly, A. Megrant, D. Sank, E. Jeffrey, Y. Chen, Y. Yin, B. Chiaro, J. Mutus, C. Neill, P. O’Malley, P. Roushan, J. Wenner, T. C. White, A. N. Cleland, and J. M. Martinis, *Phys. Rev. Lett.* **111**, 080502 (2013).
- ²³ A. Megrant, C. Neill, R. Barends, B. Chiaro, Y. Chen, L. Feigl, J. Kelly, E. Lucero, M. Mariantoni, P. J. J. O’Malley, D. Sank, A. Vainsencher, J. Wenner, T. C. White, Y. Yin, J. Zhao, C. J. Palmstrøm, J. M. Martinis, and A. N. Cleland, *Appl. Phys. Lett.* **100**, 113510 (2012); M. Reagor, H. Paik, G. Catelani, L. Sun, C. Axline, E. Holland, I. M. Pop, N. A. Masluk, T. Brecht, L. Frunzio, M. H. Devoret, L. Glazman, and R. J. Schoelkopf, *Appl. Phys. Lett.* **102**, 192604 (2013).
- ²⁴ D. F. Walls and G. J. Milburn, *Quantum Optics*, 2nd Ed. (Springer) (2006).
- ²⁵ J. E. Mooij, T. P. Orlando, L. Levitov, L. Tian, C. H. van der Wal, and S. Lloyd, *Science* **285**, 1036 (1999); T. P. Orlando, J. E. Mooij, L. Tian, C. H. van der Wal, L. S. Levitov, S. Lloyd, and J. J. Mazo, *Phys. Rev. B* **60**, 15398 (1999).
- ²⁶ J. Bylander, S. Gustavsson, F. Yan, F. Yoshihara, K. Harrabi, G. Fitch, D. G. Cory, Y. Nakamura, J.-S. Tsai, and W. D. Oliver, *Nat. Phys.* **7**, 565 (2011).
- ²⁷ T. Niemczyk, F. Deppe, H. Huebl, E. P. Menzel, F. Hocke, M. J. Schwarz, J. J. Garcia-Ripoll, D. Zueco, T. Hümmer, E. Solano, A. Marx, R. Gross, *Nat. Phys.* **6**, 772 (2010).